

Towards an Improved Ensemble Precipitation Forecast: A Probabilistic Post-Processing Approach

Sepideh Khajehei and Hamid Moradkhani

Abstract

Recently, ensemble post-processing (EPP) has become a commonly used approach for reducing the uncertainty in forcing data and hence hydrologic simulation. The procedure was introduced to build ensemble precipitation forecasts based on the statistical relationship between observations and forecasts. More specifically, the approach relies on a transfer function that is developed based on a bivariate joint distribution between the observations and the simulations in the historical period. The transfer function is used to post-process the forecast. In this study, we propose a Bayesian EPP approach based on copula functions (COP-EPP) to improve the reliability of the precipitation ensemble forecast. Evaluation of the copula-based method is carried out by comparing the performance of the generated ensemble precipitation with the outputs from an existing procedure, i.e. mixed type meta-Gaussian distribution. Monthly precipitation from Climate Forecast System Reanalysis (CFS) and gridded observation from Parameter-Elevation Relationships on Independent Slopes Model (PRISM) have been employed to generate the post-processed ensemble precipitation. Deterministic and probabilistic verification frameworks are utilized in order to evaluate the outputs from the proposed technique. Distribution of seasonal precipitation for the generated ensemble from the copula-based technique is compared to the observation and raw forecasts for three sub-basins located in the

25 Western United States. Results show that both techniques are successful in producing reliable
26 and unbiased ensemble forecast, however, the COP-EPP demonstrates considerable
27 improvement in the ensemble forecast in both deterministic and probabilistic verification, in
28 particular in characterizing the extreme events in wet seasons.

29 Post-Processing; Precipitation; Copulas; Climate Forecast System; Hydrologic Forecasting

30 **1. Introduction**

31 Uncertainty in hydrologic simulation and forecast arises from the uncertainties associated with
32 the forcing data, parameters, initial condition, and hydrologic model structure. To achieve
33 accurate hydrologic forecasts, each of these components should be estimated accurately. In the
34 past few years, researchers have proposed various techniques to tackle uncertainty in hydrologic
35 modeling from different angles. For instance, data assimilation is often proposed to deal with the
36 uncertainty in the initial and boundary conditions (DeChant and Moradkhani, 2014; Li et al.,
37 2009; Zehe and Blöschl, 2004). The skill of forecasts can be enhanced by post-processing
38 through multi-modeling (Duan et al., 2007; Madadgar and Moradkhani, 2014a; ; Najafi and
39 Moradkhani, 2015), or other statistical methods, such as quantile mapping or non-parametric
40 procedures (Madadgar et al., 2014; Wood and Schaake, 2008; Zhao et al., 2011; Zhao et al.,
41 2015); Generalized Linear Model Post-Processor (GLMPP) (Ye et al., 2014; Zhao et al., 2011);
42 and the combination of data assimilation and post processing (Bourgin et al., 2014). In addition,
43 characterizing uncertainty in forcing data has received attention in recent years (Clark and Vrugt,
44 2006; Kavetski et al., 2006; Raleigh et al., 2015; Steinschneider et al., 2012). Moreover,
45 techniques have been developed for generating ensemble meteorological forecasts (Clark et al.,
46 2004; Clark and Hay, 2004; Robertson et al., 2013; Schaake et al., 2007; Tao et al., 2014; Wu et

47 al., 2011; Zhao et al., 2011). Ensemble precipitation forecasts provide the forecasts of the most
48 likely events as well as the uncertainty information. (Park et al., 2008; Tao et al., 2014).

49 Products from the National Centers for Environmental Prediction (NCEP) models are available
50 in a diverse range of spatial and temporal scales. For instance, Short Range Forecast System
51 (SREF), Global Ensemble Forecast System (GEFS), and Climate Forecast System (CFS) are
52 widely utilized in various studies (Kumar et al., 2012; Peng et al., 2013; Wang et al., 2014).
53 Despite all of these developments in climate models, forecasts are still prone to bias in the mean
54 and insufficient spread (Hamill and Whitaker, 2006; Hamill et al., 2006; Robertson et al., 2013;
55 Tao et al., 2014; Wu et al., 2011). These errors are more significant in climate variables, such as
56 precipitation, which are affected immensely by changes in spatial scale. Thus, it is recommended
57 to not employ the ensemble products from climate models directly, due to three main reasons: 1)
58 there is low accuracy in the ensemble climate forecasts, 2) The models are developed with
59 various assumptions which may not necessarily hold for every regions, and 3) models are mostly
60 developed for large scale applications, and therefore, even if the variables are free from error at
61 their original scale, they might be biased at the catchment scale (Rayner et al., 2005; Tao et al.,
62 2014; Wu et al., 2011) .

63 There is a demand for methods that are able to generate reliable ensemble forecasts for
64 hydrologic applications. A promising approach is to apply statistical procedures to generate
65 ensemble forecast from Numerical Weather Prediction (NWP) -generated single-value forecasts.
66 The procedure is based on the bivariate probability distribution between the observation and the
67 single-value precipitation forecast. In the past few years, various methods were applied to meet
68 this objective. Kelly and Krzysztofowicz (1997) developed a bivariate meta-Gaussian
69 distribution function based on a normal quantile transformation of two variables according to the

70 Gaussian law in the Bayesian Forecasting System (BFS). The method was later used by
71 Krzysztofowicz and Herr (2001) to assess the uncertainty in the precipitation data. Clark and
72 Hay (2004) employed Model Output Statistics (MOS) to downscale the model outputs of Global
73 Forecast System (GFS), a medium range forecast system, developed in the National Weather
74 Service (NWS) cooperative network. To preserve and represent space-time variability of climate
75 variables, Clark et al. (2004) introduced a procedure, the so called Schaake Shuffle
76 reconstructing the ensemble members according to the historical values. Schaake et al. (2007)
77 described a full procedure, which is used at the National Weather Service River Forecasting
78 System (NWSRFS) for developing the ensemble meteorological forecasts as the input to the
79 ESP. It is based on the mixed distribution of the two variables and applying the normal quantile
80 transformation for building the joint distribution between the two non-normal variables. In
81 addition to the above mentioned methods, Linear Regression methods have been employed in
82 various studies to post-process precipitation at different temporal and spatial scales (Roulin &
83 Vannitsem, 2012; Sumner, Homar, & Ramis, 2001; Wilks, 2009).

84 Recently, Wu et al. (2011) developed the Mixed type meta-Gaussian joint distribution built upon
85 the method of Kelly and Krzysztofowicz (1997), which models the precipitation intermittency
86 decisively in comparison to the Schaake et al. (2007) method, which models each of the marginal
87 distributions as a convex combination of the continuous distributions. Robertson et al. (2013)
88 used the Bayesian Joint Probability approach (BJP) developed by Wang and Robertson (2011),
89 and Wang et al. (2009) for generating the ensemble precipitation forecast for a sub-daily weather
90 forecast in Australia. The number of parameters is one of the challenges in EPP; therefore, one of
91 the merits of BJP is that it uses a lesser number of parameters. Tao et al. (2014) employed EPP in
92 combination with multi-modeling to generate a more reliable forecast from The Observing

93 System Research and Predictability Experiment (THORPEX) Interactive Grand Global
94 Ensemble (TIGGE) products.

95 According to the above methods, it is assumed that the joint probability distribution between the
96 observations and the forecasts is following a multivariate normal distribution. Furthermore, using
97 normal joint distribution leads to the necessity for a transformation of the non-Gaussian variable
98 into the normal space. The transformation may affect the accuracy of the estimated probability
99 distribution (Brown and Seo, 2013; Madadgar and Moradkhani, 2014a). Therefore, Brown and
100 Seo (2013) introduced a nonparametric probability distribution. Also, Madadgar et al. (2014)
101 demonstrated that the nonparametric probability distributions are highly dependent on the
102 number of thresholds for observed variables. Consequently, it is beneficial to develop a
103 procedure that can capture the uncertainty in a way that there would be no need for variable
104 transformation, and simultaneously adopt a true probability distribution between observation and
105 forecast. Sklar (1959) introduced the concept of constructing multivariate distributions using
106 copulas. Copula functions are useful in capturing the dependency in most of the multivariate
107 distributions such as, bivariate Pareto and bivariate gamma. Copula functions have the capability
108 to draw the joint distribution regardless of the marginal distribution (Favre et al., 2004; Joe,
109 1997). Copula functions have been used substantially in hydrological applications including
110 precipitation estimation and drought forecasting (Bárdossy, 2006; Bárdossy and Pegram, 2013;
111 Bárdossy and Pegram, 2014; Dung et al., 2015; Favre et al., 2004; Madadgar and Moradkhani,
112 2013; Madadgar and Moradkhani, 2014b; Salvadori and De Michele, 2010). Madadgar et al.
113 (2014) proposed copula functions to construct the joint distribution between two variables with
114 any level of dependency because they have the potential to be applicable in post-processing the
115 hydrological simulation based on the observation and modeled streamflow simulations. They

116 showed that the copula-based method could provide a more accurate and skillful forecast in
117 comparison to the quantile mapping approach, a widely-used post-processing method.

118 In this study, we evaluate the capability of copula functions to build the joint distribution
119 between the observation and climatological forecast. This paper is organized in five sections.
120 The introduction is followed by methodology in Section 2, which includes a description of the
121 two techniques that are used in the study, as well as the forecast verification metrics that are
122 employed to evaluate the generated forecasts. Section 3 describes the data and study area.
123 Results and discussion are elaborated in Section 4, and finally, the summary and conclusion are
124 provided in Section 5.

125 **2. Methodology**

126 The main assumptions in post-processing the forecasts are that the observation and forecast are
127 correlated, and that future behavior of the system will remain the same. The purpose of this study
128 is to integrate copula functions into the EPP framework. Copula functions relax these
129 assumptions, and are able to build ensemble forecasts based on historical observations and
130 climatological forecasts. To assess the robustness and reliability of this new technique, results
131 are compared with the outputs from an existing approach called Mixed type Bivariate meta-
132 Gaussian distribution (MBG), introduced by Wu et al. (2011). The theory of copula functions is
133 provided below.

134 **2.1. Data classification and Marginal Distribution**

135 The dataset is divided into twelve monthly classes, and the procedure is applied to each class
136 separately. The procedure starts with fitting different marginal distributions to the observations
137 and forecasts. These distributions include Weibull, Exponential, Lognormal, and Gamma, which
138 are well suited to non-negative data (i.e. precipitation in this case). Furthermore, they are

139 powerful in representing the extreme values of precipitation data. To find the best marginal
 140 distribution that can describe the observation and forecast values, Bayesian Information Criterion
 141 (BIC) and Kolmogorov-Smirnov (K-S) tests are employed. For a detailed description of these
 142 tests, readers are referred to Aho et al. (2014), Raftery (1986), and Stephens (1974).

143 **2.2. Bivariate Meta-Gaussian Distribution (MBG) Approach**

144 Here we discuss generating ensembles through the MBG method (Wu et al., 2011). The goal of
 145 this approach is to build the joint cdf of two variables, the observation (O), and the forecast (Y),
 146 and then perform sampling from this cdf to generate the ensemble members at each time step.

$$F(y, o) = P(Y \leq y, O \leq o) \quad (1)$$

147 Since the joint cdf is going to be built based on the bivariate meta-Gaussian distribution,
 148 probability distribution of observation and forecast requires to be transformed into normal space.
 149 Normal Quantile Transform (NQT) is employed to derive W and Z as the replacements of F(O)
 150 and F(Y), the cdfs of observation and forecast in the normal space, respectively.

$$Z = Q^{-1}(F(Y)) \quad (2)$$

$$W = Q^{-1}(F(O)) \quad (3)$$

151 Where, Q denotes the standard normal distribution function.

152 **2.2.1. Building and Sampling from the Conditional Joint Distribution**

153 In this step, the conditional distribution between the observation and forecast is formed. By
 154 replacing the y and o by z and w respectively, it is assumed that the joint distribution between
 155 observation and forecast would be equal to the bivariate normal joint distribution between z and
 156 w ($B(z, w; \rho)$):

$$H(y, o; \rho) \equiv B(z, w; \rho) \quad (4)$$

157 where $H(y, o; \rho)$ is the bivariate meta-Gaussian distribution of Y and O , as introduced by Kelly
 158 and Krzysztofowicz (1997), and ρ is the Pearson product-moment correlation coefficient
 159 between Z and W . It can be assumed that:

$$F(y, o) \approx H(y, o; \rho) \quad (5)$$

160 According to the meta- Gaussian distribution of O and Y , the conditional distribution of O given
 161 $Y=y$ can be written as follows:

$$H(O|Y = y) = Q\left(\frac{w - \rho z}{(1 - \rho^2)^{\frac{1}{2}}}\right) \quad (6)$$

162 To create the ensemble forecast at each time step, Equation (6) is being solved employing
 163 stratified sampling of the observation given forecast, and therefore we have $p = H(O_{samples}|y)$.
 164 The ensemble members will be generated by following the Equation (7) at each p-probability.

$$Member_p = F_o^{-1}\left(Q\left(\rho z + (1 - \rho^2)^{\frac{1}{2}}Q^{-1}(p)\right)\right) \quad (7)$$

165 2.2.2. The Schaake Shuffle

166 To represent temporal dependence, the Schaake Shuffle is used to shuffle the ensemble members
 167 at each time step according to the historical observation. In this technique, the ensemble
 168 members are being ranked and matched with the historical data for the same month in the past.
 169 Then, the members will be reordered to follow the same order as the one for the historical data
 170 (Clark et al., 2004).

171 **2.3. Ensemble Post-Processing Based on Copula Functions (COP-EPP)**

172 **2.3.1. The Theory of Copula Functions**

173 Copula functions were introduced by Sklar (1959) as functions in the unit cube, which can link
174 multi-dimensional distributions to their one-dimensional marginals. Mathematically, the n-
175 dimensional copula C is represented as: $C: [0,1]^n \rightarrow [0,1]$.

176 In the bivariate case, a copula satisfies the following property:

$$C(u_1, u_2) + C(v_1, v_2) - C(u_1, v_2) - C(v_1, u_2) \geq 0 \text{ if } u_1 \geq v_1 \text{ and } u_2 \geq v_2 \quad (8)$$

177 Where u and v are the marginal distributions of two random variables. In n-dimensional space,
178 the original cumulative distribution can be written as:

$$F(x_1, x_2, \dots, x_n) = C[F_{X_1}(x_1), F_{X_2}(x_2), \dots, F_{X_n}(x_n)] = C(u_1, u_2, \dots, u_n) \quad (9)$$

$$C(u_1, u_2, \dots, u_n) = Pr\{U_1 \leq u_1, \dots, U_n \leq u_n\} \quad (10)$$

181 Based on the derivative of cumulative density function (cdf) of the copula, the probability
182 distribution function (pdf) of copula is obtained:

$$c(u_1, \dots, u_n) = \frac{\partial^n C(u_1, \dots, u_n)}{\partial u_1 \dots \partial u_n} \quad (11)$$

183 The joint density function can then be written as follows:

$$f(x_1, \dots, x_n) = c(u_1, \dots, u_n) \prod_{i=1}^n f_{X_i}(x_i) \quad (12)$$

185 There are several types of copula functions (Nelsen, 1999). Two of these families are applicable
186 in hydrology, Archimedean and Elliptical (Nelsen, 1999; Sklar, 1959). In this study, five copula
187 functions have been used: Gaussian and “t” from Elliptical, and Frank, Clayton, and Gumbel
188 from Archimedean categories.

189 To find the best copula function that describes the relationship between observations and
 190 forecasts, we use Goodness of Fit (GoF) test statistics based on the distance between the
 191 empirical and parametric copula described by Genest et al. (2009). Cramer-von Mises and
 192 Kolmogorov-Smirnov statistics were used for measuring the distance (Anderson, 1962):

$$S_n = \int_u \Delta C_n(n)^2 dC_n(u) \quad (13)$$

$$\Delta C_n = \sqrt{n}(C_n - C_{\theta_n}) \quad (14)$$

193 Where C_n is the empirical copula with sample size of n , and C_{θ_n} is the theoretical copula
 194 estimated for a sample size of n . The null hypothesis assumes that the theoretical copula fits the
 195 data. Therefore, the copula function with the greatest p-value ($p > 0.05$) and smallest S_n is desired.
 196 To calculate the p-value, parametric bootstrap procedure with 1000 iterations and $\alpha = 0.01$ is used.
 197 In this manner, the p-value is calculated as number of times that $S_{n\text{-bootstrap}}$ is greater than S_n
 198 divided by the number of iterations. In this study, we have used Inference Functions for Margins
 199 (IFM) to estimate the parameters of copula functions (Dupuis, 2007; Joe, 1997).

200 2.3.2. Ensemble Construction Based on Copula Functions

201 Ensemble members are generated by sampling from the conditional pdf of the observation given
 202 forecast at each time step. In a Bayesian network, the joint distribution of observation and
 203 forecast can be simplified as follows:

$$f(y, o) = f(y) \cdot f(o|y) \quad (15)$$

204 From Equation (15), the conditional probabilities can be derived as:

$$f(o|y) = \frac{f(o, y)}{f(y)} \quad (16)$$

205 By using copula functions in estimating the joint pdf (Equation (12)), the conditional pdf
 206 (Equation (16)) can be decomposed to a simpler form as:

$$f(s_t|y_t) = \frac{c(U_s = u_s, U_Y = u_y)f(y_t)f(s_t)}{f(y_t)} = c(U_s = u_s, U_Y = u_y)f(s_t) \quad (17a)$$

207 where $f(s_t|y_t)$ is the conditional pdf of the sample and forecast at time t, $f(y_t)$ and $f(s_t)$ are
 208 the marginal pdf of the forecast, and the sample from the observation at time t. $c(.,.)$ is the
 209 copula pdf (Madadgar et al., 2014).

210 The conditional pdf ($f(S|y_t)$) is built by Monte Carlo sampling from the copula density
 211 function ($c(U_s, U_Y = u_y)$), in the following steps: 1) The forecast is fixed at time t ($U_Y = u_y$ at
 212 time t), 2) Generate U_s by sampling from the historical observation (500 samples in this study).
 213 3) compute the value of $c(U_s, U_Y = u_y)$. Now Equation (17a) is modified as follows:

$$f(S|y_t) = c(U_s, U_Y = u_y)f(s) \quad (17b)$$

214 Following Schaake et al. (2007), to sample from the conditional pdf and to generate the
 215 ensemble of size n (in this study, 20) the probabilities at equal intervals (0.05, 0.1, 0.15, ..., 0.95)
 216 are considered. Then, the ensemble members associated with above probabilities are obtained.
 217 To preserve the temporal variability, the Schaake Shuffle is used to shuffle the ensemble
 218 members at each time step according to the historical observation. Figure 1 demonstrates the
 219 schematic of COP-EPP procedure.

220 **Figure 1.** Schematic of the Copula-based ensemble post-processing (COP-EPP). The ensemble
 221 members are generated by sampling from conditional pdf and reconstructed according to
 222 Schaake shuffle.

223 2.4. Forecast Verification

224 To examine the robustness, reliability, and effectiveness of the proposed approach, results of
225 both approaches, i.e. MBG and COP-EPP are compared through deterministic and probabilistic
226 verification metrics. Accordingly, one deterministic and two probabilistic measures are chosen to
227 evaluate the two generated ensembles. To have a clear comparison between results, normalized
228 measures are employed. For sufficient examination of results, the generated ensembles are
229 analyzed during both the calibration and verification periods.

230 2.4.1. Deterministic Measures

231 To inspect the errors in the mean ensemble precipitation forecast, deterministic measures are
232 used. Also, it would be beneficial to study the relationship between the observation and raw
233 forecast in a deterministic framework.

234 Absolute Percent bias evaluates the deviation of the ensemble mean from the observation. The
235 optimal value of Absolute percent bias is zero (Gupta, Sorooshian, & Yapo, 1999; Moriasi et al.,
236 2007).

$$\text{Absolute Percent Bias} = \frac{\sum_{i=1}^n |y_i - o_i|}{\sum_{i=1}^n (o_i)} \times 100 \quad (18)$$

237 To assess the accuracy of the forecast versus observation, the Kling-Gupta Efficiency (KGE)
238 measure is utilized. KGE was introduced as the modified version of Nash-Sutcliffe Efficiency
239 (NSE) by Gupta et al. (2009). This measure captures the correlation, bias, and variability in the
240 forecast data versus the observation.

$$KGE = 1 - ED \quad (19)$$

$$ED = \sqrt{(r - 1)^2 - (\alpha - 1)^2 - (\beta - 1)^2} \quad (120)$$

241 ED is defined as the Euclidean distance between two variables, r represents the linear correlation
 242 coefficient between the observation and forecast, α is the ratio of variance of forecast to variance
 243 in observation (relative variability in the forecast and observation), and β represents the ratio
 244 bias. ED is always non-negative, and thus KGE will have a value from $-\infty$ to 1, with optimal
 245 value of 1.

246 **2.4.2. Probabilistic Measures**

247 Since the deterministic measures are affected by over or under -confident forecasts, it is essential
 248 to examine the generated forecast through probabilistic measures as well. Probabilistic measures
 249 are beneficial in assessing the reliability of ensemble forecast (DeChant and Moradkhani, 2014b;
 250 DeChant and Moradkhani, 2015). To assess the forecast skill of the generated ensembles,
 251 Continuous Ranked Probability Skill Score (CRPSS) is employed. This measure is the
 252 normalized version of Continuous Ranked Probability Score (CRPS) that has been introduced as
 253 the extension of Brier Score over all the possible thresholds (Hersbach, 2000).

$$CRPS = \int_{x=-\infty}^{x=\infty} (F^y(x) - F_o(x))^2 dx \quad (21)$$

254 and

$$F_o(x) = \begin{cases} 0, & x < \text{observed value} \\ 1, & x \geq \text{observed value} \end{cases} \quad (22)$$

255 Where $F^{fo}(x)$ is the forecast probability, i.e. cdf of the forecast . In the deterministic case CRPS
 256 will be the same as MAE with the optimal value of zero.

$$CRPSS = \frac{\overline{CRPS_{ref}} - \overline{CRPS_{forecast}}}{\overline{CRPS_{ref}}} \quad (23)$$

257 CRPS_{ref} refers to the Continues Ranked Probability Score for the observation. The range for
 258 CRPSS is $-\infty$ to one with optimal value of one.

$$259 \quad CRPS_{ref} = \frac{1}{T} \sum_{t=1}^T \sum |o(t) - \bar{o}| \quad (24)$$

260 One of the techniques used to evaluate the forecast skill is to employ the Relative (or Receiver)
 261 Operating Characteristic (ROC) curve in which the hit rate and false- alarm are compared
 262 (Mason, 1982). The area under the curve represents the ROC score ranging between 0 and 1 with
 263 the perfect score of 1. In this study, the ROC score is used to examine the resolution of the
 264 generated forecast for winter precipitation (December, January, and February) during the
 265 verification period (2000-2014).

266 The ROC score is not sensitive to bias in the forecast (Wilks, 2011); therefore, it can be
 267 considered as a measure for assessing the potential usefulness of a certain forecast. On the
 268 contrary, bias can affect the reliability of forecast (Murphy, 1993). Accordingly, the reliability of
 269 winter precipitation is evaluated based on the decomposition of the Brier score (Murphy, 1993)
 270 and calculating the reliability at threshold of a 95 percentile of the observation as follows:

$$271 \quad Reliability = \frac{1}{T} \sum_{b=1}^B n_b (\bar{p}_b - \bar{O}_b)^2 \quad (25)$$

272 To calculate the reliability, it is important to group the forecasts into B forecast bins. Each bin
 273 has a population of n_b , with an average forecast probability of \bar{p}_b and an observed frequency of
 274 \bar{O}_b . For more details about reliability, readers are encouraged to refer to (Wilks, 2011).

275 **3. Data and Study Area**

276 The applicability and usefulness of the methods are evaluated over three basins located in the
277 Western United States, as shown in Figure 2. The characteristics of each of these three basins are
278 summarized in Table 1.

279 **Figure 2.** The location of three study basins in the Western USA.

280 **Table 1.** Summary characteristics of the study basins.

281 This study is conducted on monthly precipitation over the historical period (1979-2014). The
282 first twenty-one years are used to calibrate the model, followed by fifteen years of validation
283 period. The observation dataset is extracted from the Parameter-Elevation Relationships on
284 Independent Slopes Model (PRISM) Climate Group, <http://prism.oregonstate.edu>. The observed
285 precipitation includes rainfall and melted snow over 4km grid cells.

286 Climate Forecast System Reanalysis (CFSR) and Climate Forecast System version 2 (CFSv2)
287 developed by the National Centers for Environmental Prediction (NCEP) are utilized as the
288 climatologic forecast (Saha et al., 2010; Saha et al., 2014). The six-hourly precipitation at 0.5° spatial
289 resolution is chosen and accumulated to the monthly values for evaluation of forecast.

290 To prepare the datasets for this study, the observation dataset is re-gridded to $0.5^\circ \times 0.5^\circ$
291 resolution.

292 **4. Results and Discussion**

293 **4.1. Raw Forecast Validation**

294 We begin by evaluating the relationship between the raw forecast and the observation. In order to
295 achieve this objective, KGE is calculated for the raw forecast in relation to the observation for
296 calibration period. Results are shown in Figure 3.

297 **Figure 3.** Kling-Gupta efficiency measure for the raw forecast during calibration period. White
298 grid cells in Rouge River Basin present missing observations.

299 The acceptable range for KGE is considered to be above 0.6; therefore, results in Figure 3 show
300 that the raw forecast does not have good skill as compared with the observation. More
301 specifically, results show that the KGE is less than 0.6 for the major portion of all three basins,
302 indicating that the observation mean is better in describing the precipitation event in comparison
303 to the raw forecast. The above inspections lead to the conclusion that it is not appropriate to use
304 the raw forecast.

305 **4.2. Selection of Copula Functions**

306 The experiment starts with finding the best copula function that describes the joint distribution
307 between the observation and the forecast during the calibration period. As an example, Figure 4
308 presents copula functions that successfully map the joint distribution for each month in each grid
309 cell in the upper Colorado River Basin. The figure demonstrates that among the copula functions
310 used in this basin, the Frank copula provides the best fit in describing the joint distribution
311 between the observation and the raw forecast in most months. Further inspection reveals that this
312 pattern is not followed for some of the months. As seen in Figure 4, the Clayton and T Copulas
313 are the most chosen distributions in March. In June, Gumbel and T-Copula are the dominant
314 copula functions chosen.

315 **Figure 4.** Selection of suitable copula functions for each grid cell across the Upper Colorado
316 River Basin.

317 According to Figure 4, copula functions will be fitted, and ensemble members will be built from
318 the conditional pdf of sample variable given the raw forecast at each time step. Here, the
319 ensemble precipitation forecast with twenty members will be generated.

320 4.3. Deterministic Verification

321 The Absolute percent bias calculated for the study period (1979-2014) is presented in Figure 5.
322 This Figure demonstrates the calculated Absolute percent bias distribution over the study basins
323 for raw forecast and the bias-corrected ensemble means (i.e. MBG and COP-EPP). The highest
324 bias for the raw forecast is found in the Upper Colorado basin where Absolute percent bias
325 ranges from 50% to 300%. Both techniques improve the accuracy of the raw forecast by more
326 than 50%. The improvement is more considerable in Rogue basin, where the average of the
327 Absolute percent bias over the basin is reduced from 150% to 80% and 60% for MBG and COP-
328 EPP methods, respectively. COP-EPP method shows to be more effective in reducing the bias as
329 compared to MBG method. Overall, there is a 20% difference between the two techniques across
330 the study basins.

331 **Figure 5.** Absolute percent bias distribution over the three study basins. The bias is calculated
332 for the raw forecast (blue line), and the ensemble mean from the MGB and COP-EPP outputs
333 (red and green lines, respectively).

334 Results are evaluated with the KGE metric, which is a deterministic measure. A deterministic
335 comparison has been done on the ensemble means of both methods in calibration and validation
336 periods.

337 Figure 6 shows the KGE results in the calibration and the validation periods for each study basin.
338 Figures 3 and 6 show a significant improvement in generated forecast ensemble as compared to
339 the raw precipitation forecast. In addition, COP-EPP shows about 10% higher KGE values than
340 that of MBG during the calibration period. This is more significant for the validation period
341 where the range of calculated KGE for COP-EPP is always larger than that of MBG.
342 Furthermore, the discrepancy between the validation and the calibration period is less significant

343 in the COP-EPP method than in the MBG method. For instance, in the Rogue River Basin, the
344 calculated KGE for the MBG method shows a decrease of 20% when compared with its
345 calibration results; while this is not the case for COP-EPP. In the Upper Colorado Basin, the
346 MBG method results in KGE values are less than 0.6 in some grids, which may not be
347 considered accurate enough in some specific studies (Bisselink, Zambrano-Bigiarini, Burek, &
348 de Roo, 2016; Thiemig, Rojas, Zambrano-Bigiarini, & De Roo, 2013).

349 **Figure 6.** KGE measure calculated over the study basins after post-processing using the COP-
350 EPP and MBG methods during calibration (left) and verification (right) periods.

351 **4.4. Probabilistic Verification**

352 Figure 7 shows the results for the probabilistic verification of the ensemble forecast generated by
353 each method in each basin. This figure presents the CRPSS analysis for both the calibration and
354 the validation periods. The results of the CRPSS analysis demonstrate a significant improvement
355 of the raw forecast after EPP in both techniques, with a more significant improvement based on
356 COP-EPP. During the calibration period, the copula method shows superior results by almost
357 10% in comparison to the MBG's results in all basins, whereas in Rogue River Basin, disparity
358 in the MBG results is slightly higher, indicating that in basins with higher precipitation, COP-
359 EPP is more successful than MBG in generating more skillful ensemble forecasts.

360 Figure 7 indicates that both methods result in higher values of CRPSS in the western parts of
361 Upper Colorado River Basin. For central parts of Southern Snake Basin, CRPSS shows the
362 lowest values for the generated ensemble precipitation compared to the observation.
363 Significantly, the spatial pattern is maintained in the validation period for both techniques in all
364 the basins.

365 Comparing the results for both techniques in the validation period indicates that copula outputs
366 are more successful in preserving the accuracy of the generated ensemble in this period. For
367 instance, in the case of Rogue River Basin, CRPSS is reduced by almost 2% in the validation
368 period compared to the calibration for COP-EPP outputs. Meanwhile, this difference is about
369 10% for MBG results. This schema is visible for the other two basins with less noticeable
370 difference.

371 **Figure 7.** CRPSS measure calculated for 3 basins after implementing two post-processing
372 methods for the calibration (left) and verification (right) periods.

373 The ROC scores are presented in Figure 8. Both post-processing methods maintain a ROC score
374 above 0.5, which is an encouraging outcome for the generated ensemble forecast. Comparing the
375 results from the Southern Snake and Upper Colorado basins shows that COP-EPP generates the
376 ensemble forecast with higher resolution than that of the MBG method. The difference between
377 the two methods is more noticeable in Rogue River Basin, which receives relatively higher
378 precipitation than the other basins.

379 **Figure 8.** Assessment of forecast resolution based on ROC score for winter (Dec, Jan, and Feb)
380 precipitation during verification period (2001-2014).

381 Since the focus of this study is to minimize the bias in the forecast, in addition to resolution,
382 reliability of the generated forecast is evaluated for each basin. According to the formulation of
383 reliability (eq. 21), the lower the score the more reliable the ensemble forecast will be. Figure 9
384 illustrates that COP-EPP has a reliability score of less than 0.05 for approximately all the grid
385 cells in the three basins. Although, in general, the MBG method, provides a reliable ensemble
386 forecast across the basins, the COP-EPP shows noticeably better performance than the MBG .
387 Since the reliability of the forecasts is examined for the ninety-fifth percentile of the observation,

388 this can also indicate the reliability of the generated forecasts on the extremes. Although both
389 methods are shown capable of detecting the extremes, the COP-EPP demonstrates more accuracy
390 on extreme values.

391 **Figure 9.** Reliability measure for winter precipitation (Dec, Jan, and Feb) calculated at 95th
392 percentile of observation during the verification period (2001-2014). This measure ranges from 0
393 to 1 with the optimal value of 0.

394 **4.5. Seasonal Evaluation of the Generated Ensemble Forecasts**

395 To study the performance of the generated ensemble precipitation based on the COP-EPP,
396 seasonal precipitation is evaluated for each basin. Accordingly, the most probable ensemble
397 member (the mode of the conditional pdf), which can substitute the raw forecast as a better
398 predictor, is chosen for this purpose. For a clear inspection, the spatial average of the most
399 probable ensemble member is utilized over the study basin.

400 Results of seasonal assessment are summarized in Figure 10. In the figure, the observation is
401 shown by the green line, the raw forecast is shown by the red line, the blue line displays the most
402 probable ensemble member from the generated ensemble forecast by COP-EPP, and the black
403 line represents the indicated ensemble member from MBG's generated forecast. Overall, the
404 post-processed forecast shows a significant improvement in describing seasonal precipitation
405 distribution in comparison to the raw forecast. For an instance, in the spring, the precipitation
406 distribution from the raw forecast (red line) overestimates the observation (green line), whereas
407 the COP-EPP forecast almost follows the same distribution as the observation. In summer, the
408 raw forecast distribution shows better performance compared to other seasons. On the other
409 hand, in a severe condition such as Rogue River Basin, which is a coastal region, the raw

410 forecast is not able to follow the observation's distribution. This is more noticeable in winter
411 when basins receive more precipitation.

412 Seasonal results for the Upper Colorado Basin, a semi-arid region, demonstrate no significant
413 difference between precipitations in different seasons whereas in the Southern Snake Basin,
414 spring and winter receive more precipitation than summer and fall. These changes become more
415 significant when a coastal basin, such as the Rogue River Basin, is studied. In inspecting the
416 results for the Upper Colorado Basin, it can be seen that the raw forecast is over-predicting the
417 observation, especially in spring and winter. This pattern is approximately the same for the
418 Southern Snake River Basin. However, in the Rogue River Basin, summers receive much less
419 precipitation compared to other seasons. Observations for this basin show the same distribution
420 pattern for a high level of precipitation in fall and spring. Results for winter in this basin show
421 much higher precipitation with an average of about 600 mm. In comparing the raw forecast with
422 the three other datasets, i.e. observation and two generated forecasts, results indicate that the raw
423 forecast has higher seasonal precipitation values in all seasons with a significant difference in
424 winter. In summer, the forecast is following the same distribution as the observation with minor
425 under-prediction for the Rogue River Basin. Furthermore, in wet seasons, the generated forecasts
426 successfully follow the observation distribution, whereas MBG is showing minor under-
427 prediction. In extreme cases, such as winter in the Rogue River Basin, the raw forecast shows a
428 large bias while COP-EPP was successful in reducing the bias, similar to spring and fall.

429 Overall, COP-EPP has shown significant potential in generating more reliable and accurate
430 ensemble forecasts. Compared to the benchmark technique, COP-EPP shows more consistency
431 in the validation period as compared to that of MBG. In the cases with extreme precipitation,
432 COP-EPP still shows superior results. Lastly, COP-EPP is robust in conserving the spatial

433 pattern of calculated measures. Generally, results show higher accuracy in wet seasons; a
434 specifically generated ensemble forecast is showing promising results in the extreme cases such
435 as winter for the Rogue River Basin.

436 Brown and Seo (2013) argue that back and forth transformation from Gaussian space can
437 invalidate the optimality of estimated parameters of the conditional probability distribution.
438 However, the improvement in the COP-EPP compared to the MBG can be attributed to the
439 procedure used by COP-EPP to model the dependence structure between observation and
440 forecast. COP-EPP joins the variables via their marginal distribution. Therefore, the complexity
441 in the hydro-meteorological processes does not constrain modeling the joint behavior of
442 observation and forecast (Dupuis, 2007; Madadgar & Moradkhani, 2014).

443 **Figure 10.** Probability density functions of seasonal precipitation from the observation, raw
444 forecast, and most probable forecast based on the COP-EPP and MBG approach for three study
445 basins. Seasonal precipitation is spatially averaged over all grid cells of each basin. Seasons are
446 categorized in the following order: Spring (Mar, Apr, and May), summer (Jun, Jul, and Aug), fall
447 (Sep, Oct, and Nov), and winter (Dec, Jan, and Feb).

448 **5. Conclusion and Summary**

449 The purpose of this study is to examine the accuracy and reliability of ensemble precipitation
450 prediction utilizing copula functions. The technique is based on the relationship between the
451 single value forecast and historical observation. Therefore, the assessment is done by comparing
452 results from the new copula method with that of a well-known procedure, MBG.

453 Comparison is undertaken by employing three different basins with semi-arid to coastal climates
454 to study the performance of the techniques in different climate regimes. Deterministic

455 verification indicates promising improvement in the mean ensemble using the COP-EPP for
456 generating ensemble precipitation forecast. In order to assess the forecast skill, probabilistic
457 measures including CRPSS, reliability, and the ROC score are employed. The results of CRPSS
458 indicate that the generated ensemble forecast from COP-EPP is more reliable and accurate in
459 comparison to the meta-Gaussian one. Furthermore, through analysis of reliability, it is noticed
460 that the copula- based method is more successful in generating the ensemble forecasts that
461 represent extremes. The ROC score indicated that both techniques are capable of generating
462 potentially useful ensemble forecasts with high resolution; however, in the basin with higher
463 precipitation (i.e., Rogue River Basin), COP-EPP proves to be even more superior.

464 Overall, both techniques show promising results, and existing procedures generated ensembles
465 with acceptable reliability. However, using copula functions will help improve the quality of
466 ensemble forecasting. COP-EPP is shown to be more precise in building the ensemble
467 precipitation forecast. In other words, results demonstrate that the copula procedure is
468 approximately independent of spatial and temporal changes in the data.

469 It is worth mentioning that incorporating copula functions into EPP helps overcome the
470 assumption of normal distribution for the observation and forecast. It is therefore possible to
471 eliminate the transformation step in EPP procedure. Moreover, copula functions are capable of
472 building joint distribution between two datasets with any level of dependency, and for any
473 marginal distributions. These characteristics of copula functions help us generate more accurate
474 ensemble forecast.

475 **Acknowledgement**

476 The authors would like to acknowledge the financial support for this study by NOAA Grants No.
477 NA11NWS4680002 and NA140AR4310234.

478 **References**

- 479 Aho, K., Derryberry, D. and Peterson, T., 2014. Model selection for ecologists: the worldviews
480 of AIC and BIC. *Ecology*, 95(3): 631-636.
- 481 Anderson, T.W., 1962. On the distribution of the two-sample Cramer-von Mises criterion. *The*
482 *Annals of Mathematical Statistics*: 1148-1159.
- 483 Bisselink, B., Zambrano-Bigiarini, M., Burek, P., de Roo, A., 2016. Assessing the role of
484 uncertain precipitation estimates on the robustness of hydrological model parameters under
485 highly variable climate conditions. *J. Hydrol. Reg. Stud.* 8, 112–129.
486 doi:<http://dx.doi.org/10.1016/j.ejrh.2016.09.003>
- 487 Bourgin, F., Ramos, M.H., Thirel, G. and Andréassian, V., 2014. Investigating the interactions
488 between data assimilation and post-processing in hydrological ensemble forecasting.
489 *Journal of Hydrology*, 519, Part D: 2775-2784.
- 490 Brown, J.D. and Seo, D.J., 2013. Evaluation of a nonparametric post-processor for bias
491 correction and uncertainty estimation of hydrologic predictions. *Hydrological Processes*,
492 27(1): 83-105.
- 493 Bárdossy, A., 2006. Copula-based geostatistical models for groundwater quality parameters.
494 *Water Resources Research*, 42(11).
- 495 Bárdossy, A. and Pegram, G., 2013. Interpolation of precipitation under topographic influence at
496 different time scales. *Water Resources Research*, 49(8): 4545-4565.
- 497 Bárdossy, A. and Pegram, G., 2014. Infilling missing precipitation records – A comparison of a
498 new copula-based method with other techniques. *Journal of Hydrology*, 519, Part A:
499 1162-1170.
- 500 Clark, M., Gangopadhyay, S., Hay, L., Rajagopalan, B. and Wilby, R., 2004. The Schaake
501 shuffle: A method for reconstructing space-time variability in forecasted precipitation and
502 temperature fields. *Journal of Hydrometeorology*, 5(1): 243-262.
- 503 Clark, M.P. and Hay, L.E., 2004. Use of medium-range numerical weather prediction model
504 output to produce forecasts of streamflow. *Journal of Hydrometeorology*, 5(1): 15-32.
- 505 Clark, M.P. and Vrugt, J.A., 2006. Unraveling uncertainties in hydrologic model calibration:
506 Addressing the problem of compensatory parameters. *Geophysical Research Letters*,
507 33(6).
- 508 DeChant, C.M. and Moradkhani, H., 2014b. Toward a reliable prediction of seasonal forecast
509 uncertainty: Addressing model and initial condition uncertainty with ensemble data
510 assimilation and Sequential Bayesian Combination. *Journal of Hydrology*, 519, Part
511 D(0): 2967-2977.
- 512 DeChant, C.M. and Moradkhani, H., 2015. On the assessment of reliability in probabilistic
513 hydrometeorological event forecasting. *Water Resources Research*.
- 514 Duan, Q., Ajami, N.K., Gao, X. and Sorooshian, S., 2007. Multi-model ensemble hydrologic
515 prediction using Bayesian model averaging. *Advances in Water Resources*, 30(5): 1371-
516 1386.
- 517 Dung, N.V., Merz, B., Bárdossy, A. and Apel, H., 2015. Handling uncertainty in bivariate
518 quantile estimation – An application to flood hazard analysis in the Mekong Delta.
519 *Journal of Hydrology*, 527: 704-717.
- 520 Dupuis, D. J. (2007). Using copulas in hydrology: Benefits, cautions, and issues. *Journal of*
521 *Hydrologic Engineering*, 12(4), 381–393.
- 522 Favre, A.C., El Adlouni, S., Perreault, L., Thiémonge, N. and Bobée, B., 2004. Multivariate

523 hydrological frequency analysis using copulas. *Water resources research*, 40(1).

524 Genest, C., Rémillard, B. and Beaudoin, D., 2009. Goodness-of-fit tests for copulas: A review
525 and a power study. *Insurance: Mathematics and economics*, 44(2): 199-213.

526 Gupta, H.V., Kling, H., Yilmaz, K.K. and Martinez, G.F., 2009. Decomposition of the mean
527 squared error and NSE performance criteria: Implications for improving hydrological
528 modelling. *Journal of Hydrology*, 377(1–2): 80-91.

529 Gupta, H.V., Sorooshian, S., Yapo, P.O., 1999. Status of automatic calibration for hydrologic
530 models: Comparison with multilevel expert calibration. *J. Hydrol. Eng.* 4, 135–143.

531 Hamill, T.M. and Whitaker, J.S., 2006. Probabilistic quantitative precipitation forecasts based on
532 reforecast analogs: Theory and application. *Monthly Weather Review*, 134(11): 3209-
533 3229.

534 Hamill, T.M., Whitaker, J.S. and Mullen, S.L., 2006. Reforecasts: An Important Dataset for
535 Improving Weather Predictions. *Bulletin of the American Meteorological Society*, 87(1):
536 33-46.

537 Hersbach, H., 2000. Decomposition of the Continuous Ranked Probability Score for Ensemble
538 Prediction Systems. *Weather and Forecasting*, 15(5): 559-570.

539 Joe, H., 1997. *Multivariate models and multivariate dependence concepts*, 73. CRC Press.

540 Kavetski, D., Kuczera, G. and Franks, S.W., 2006. Bayesian analysis of input uncertainty in
541 hydrological modeling: 2. Application. *Water Resources Research*, 42(3).

542 Kelly, K.S. and Krzysztofowicz, R., 1997. A bivariate meta-Gaussian density for use in
543 hydrology. *Stochastic Hydrology and Hydraulics*, 11(1): 17-31.

544 Krzysztofowicz, R. and Herr, H.D., 2001. Hydrologic uncertainty processor for probabilistic
545 river stage forecasting: precipitation-dependent model. *Journal of Hydrology*, 249(1): 46-
546 68.

547 Kumar, A., Chen, M., Zhang, L., Wang, W., Xue, Y., Wen, C., Marx, L. and Huang, B., 2012.
548 An analysis of the nonstationarity in the bias of sea surface temperature forecasts for the
549 NCEP Climate Forecast System (CFS) version 2. *Monthly Weather Review*, 140(9):
550 3003-3016.

551 Li, H., Luo, L., Wood, E.F. and Schaake, J., 2009. The role of initial conditions and forcing
552 uncertainties in seasonal hydrologic forecasting. *Journal of Geophysical Research:*
553 *Atmospheres* (1984–2012), 114(D4).

554 Madadgar, S. and Moradkhani, H., 2013. A Bayesian Framework for Probabilistic Seasonal
555 Drought Forecasting. *Journal of Hydrometeorology*, 14(6): 1685-1705.

556 Madadgar, S. and Moradkhani, H., 2014a. Improved Bayesian multimodeling: Integration of
557 copulas and Bayesian model averaging. *Water Resources Research*: n/a-n/a.

558 Madadgar, S. and Moradkhani, H., 2014b. Spatio-temporal drought forecasting within Bayesian
559 networks. *Journal of Hydrology*, 512: 134-146.

560 Madadgar, S., Moradkhani, H. and Garen, D., 2014. Towards improved post-processing of
561 hydrologic forecast ensembles. *Hydrological Processes*, 28(1): 104-122.

562 Mason, I., 1982. A model for assessment of weather forecasts. *Aust. Meteor. Mag.*, 30(4): 291-
563 303.

564 Murphy, A.H., 1993. What is a good forecast? An essay on the nature of goodness in weather
565 forecasting. *Weather and forecasting*, 8(2): 281-293.

566 Moriasi, D.N., Arnold, J.G., Van Liew, M.W., Bingner, R.L., Harmel, R.D., Veith, T.L., 2007.
567 Model evaluation guidelines for systematic quantification of accuracy in watershed
568 simulations. *Trans. Asabe* 50, 885–900.

569 Najafi, M.R. and Moradkhani, H., 2015. Ensemble combination of seasonal streamflow
570 forecasts. *Journal of Hydrologic Engineering*, 21(1): 04015043.

571 Nelsen, R.B., 1999. An introduction to copulas, volume 139 of Lecture Notes in Statistics.
572 Springer-Verlag, New York.

573 Park, Y.Y., Buizza, R. and Leutbecher, M., 2008. TIGGE: Preliminary results on comparing and
574 combining ensembles. *Quarterly Journal of the Royal Meteorological Society*, 134(637):
575 2029-2050.

576 Parrish, M.A., Moradkhani, H. and DeChant, C.M., 2012. Toward reduction of model
577 uncertainty: Integration of Bayesian model averaging and data assimilation. *Water*
578 *Resources Research*, 48(3): n/a-n/a.

579 Peng, P., Barnston, A.G. and Kumar, A., 2013. A comparison of skill between two versions of
580 the NCEP climate forecast system (CFS) and CPC's operational short-lead seasonal
581 outlooks. *Weather and Forecasting*, 28(2): 445-462.

582 Raftery, A.E., 1986. Choosing models for cross-classifications. *American Sociological Review*,
583 51(1): 145-146.

584 Raleigh, M.S., Lundquist, J.D. and Clark, M.P., 2015. Exploring the impact of forcing error
585 characteristics on physically based snow simulations within a global sensitivity analysis
586 framework. *Hydrol. Earth Syst. Sci.*, 19(7): 3153-3179.

587 Rayner, S., Lach, D. and Ingram, H., 2005. Weather Forecasts are for Wimps: Why Water
588 Resource Managers Do Not Use Climate Forecasts. *Climatic Change*, 69(2-3): 197-227.

589 Robertson, D.E., Shrestha, D.L. and Wang, Q.J., 2013. Post processing rainfall forecasts from
590 numerical weather prediction models for short term streamflow forecasting. *Hydrology*
591 *and Earth System Sciences Discussions*, 10(5): 6765-6806.

592 Roulin, E., & Vannitsem, S. (2012). Postprocessing of ensemble precipitation predictions with
593 extended logistic regression based on hindcasts. *Monthly Weather Review*, 140(3), 874–888.

594 Saha, S., Moorthi, S., Pan, H.-L., Wu, X., Wang, J., Nadiga, S., Tripp, P., Kistler, R., Woollen, J.
595 and Behringer, D., 2010. The NCEP climate forecast system reanalysis. *Bulletin of the*
596 *American Meteorological Society*, 91(8): 1015-1057.

597 Saha, S., Moorthi, S., Wu, X., Wang, J., Nadiga, S., Tripp, P., Behringer, D., Hou, Y.-T.,
598 Chuang, H.-y. and Iredell, M., 2014. The NCEP climate forecast system version 2.
599 *Journal of Climate*, 27(6): 2185-2208.

600 Salvadori, G. and De Michele, C., 2010. Multivariate multiparameter extreme value models and
601 return periods: A copula approach. *Water resources research*, 46(10).

602 Schaake, J., Demargne, J., Hartman, R., Mullusky, M., Welles, E., Wu, L., Herr, H., Fan, X. and
603 Seo, D.J., 2007. Precipitation and temperature ensemble forecasts from single-value
604 forecasts. *Hydrology and Earth System Sciences Discussions Discussions*, 4(2): 655-717.

605 Sklar, M., 1959. Fonctions de répartition à n dimensions et leurs marges. *Université Paris 8*.

606 Steinschneider, S., Polebitski, A., Brown, C. and Letcher, B.H., 2012. Toward a statistical
607 framework to quantify the uncertainties of hydrologic response under climate change.
608 *Water Resources Research*, 48(11).

609 Stephens, M.A., 1974. EDF statistics for goodness of fit and some comparisons. *Journal of the*
610 *American statistical Association*, 69(347): 730-737.

611 Sumner, G., Homar, V., & Ramis, C. (2001). Precipitation seasonality in eastern and southern
612 coastal Spain. *International Journal of Climatology*, 21(2), 219–247.
613 <http://doi.org/10.1002/joc.600>.

614 Tao, Y., Duan, Q., Ye, A., Gong, W., Di, Z., Xiao, M. and Hsu, K., 2014. An evaluation of post-

615 processed TIGGE multimodel ensemble precipitation forecast in the Huai river basin.
616 *Journal of Hydrology*, 519, Part D(0): 2890-2905.

617 Thiemiig, V., Rojas, R., Zambrano-Bigiarini, M., & De Roo, A. (2013). Hydrological evaluation
618 of satellite-based rainfall estimates over the Volta and Baro-Akobo Basin. *Journal of*
619 *Hydrology*, 499, 324–338.

620 Wang, Q.J. and Robertson, D.E., 2011. Multisite probabilistic forecasting of seasonal flows for
621 streams with zero value occurrences. *Water Resources Research*, 47(2): W02546.

622 Wang, Q.J., Robertson, D.E. and Chiew, F.H.S., 2009. A Bayesian joint probability modeling
623 approach for seasonal forecasting of streamflows at multiple sites. *Water Resources*
624 *Research*, 45(5): W05407.

625 Wang, W., Hung, M.-P., Weaver, S.J., Kumar, A. and Fu, X., 2014. MJO prediction in the NCEP
626 Climate Forecast System version 2. *Climate dynamics*, 42(9-10): 2509-2520.

627 Wilks, D. S. 2009. Extending logistic regression to provide full-probability-distribution MOS
628 forecasts. *Meteorological Applications*, 16(3), 361–368.

629 Wilks, D.S., 2011. *Statistical methods in the atmospheric sciences*, 100. Academic press.

630 Wood, A.W. and Schaake, J.C., 2008. Correcting errors in streamflow forecast ensemble mean
631 and spread. *Journal of Hydrometeorology*, 9(1): 132-148.

632 Wu, L., Seo, D.-J., Demargne, J., Brown, J.D., Cong, S. and Schaake, J., 2011. Generation of
633 ensemble precipitation forecast from single-valued quantitative precipitation forecast for
634 hydrologic ensemble prediction. *Journal of hydrology*, 399(3): 281-298.

635 Yan, H., DeChant, C.M. and Moradkhani, H., Improving Hydrologic Data Assimilation by a
636 Multivariate Particle Filter-Markov Chain Monte Carlo, pp. 0773.

637 Ye, A., Duan, Q., Yuan, X., Wood, E.F. and Schaake, J., 2014. Hydrologic post-processing of
638 MOPEX streamflow simulations. *Journal of Hydrology*, 508: 147-156.

639 Zehe, E. and Blöschl, G., 2004. Predictability of hydrologic response at the plot and catchment
640 scales: Role of initial conditions. *Water Resources Research*, 40(10).

641 Zhao, L., Duan, Q., Schaake, J., Ye, A. and Xia, J., 2011. A hydrologic post-processor for
642 ensemble streamflow predictions. *Advances in Geosciences*, 29(29): 51-59.

643 Zhao, T., Wang, Q.J., Bennett, J.C., Robertson, D.E., Shao, Q. and Zhao, J., 2015. Quantifying
644 predictive uncertainty of streamflow forecasts based on a Bayesian joint probability
645 model. *Journal of Hydrology*, 528: 329-340.

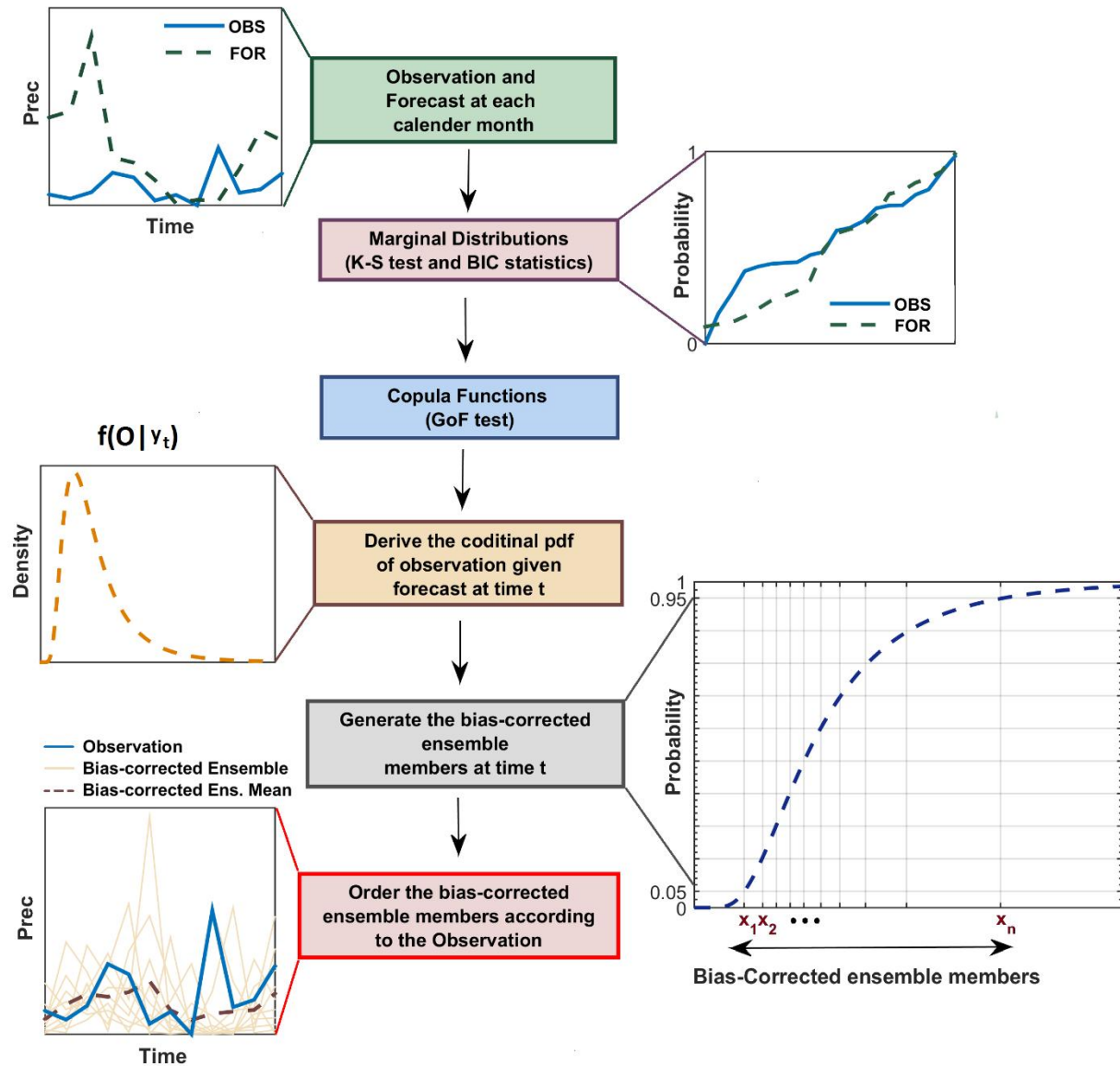


Figure 1. Schematic of the Copula-based ensemble post-processing (COP-EPP). The ensemble members are generated by sampling from conditional pdf and reconstructed according to Schaake shuffle.

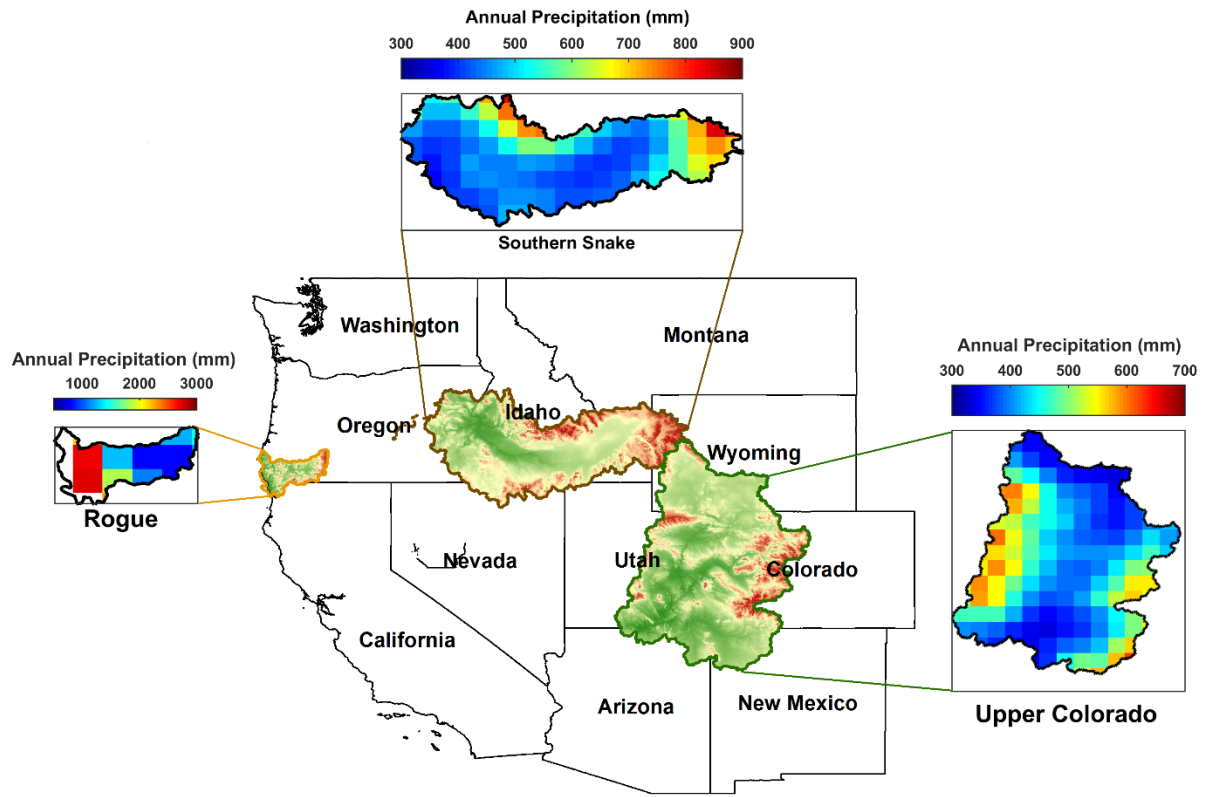


Figure 2. The location of three study basins in the Western USA.

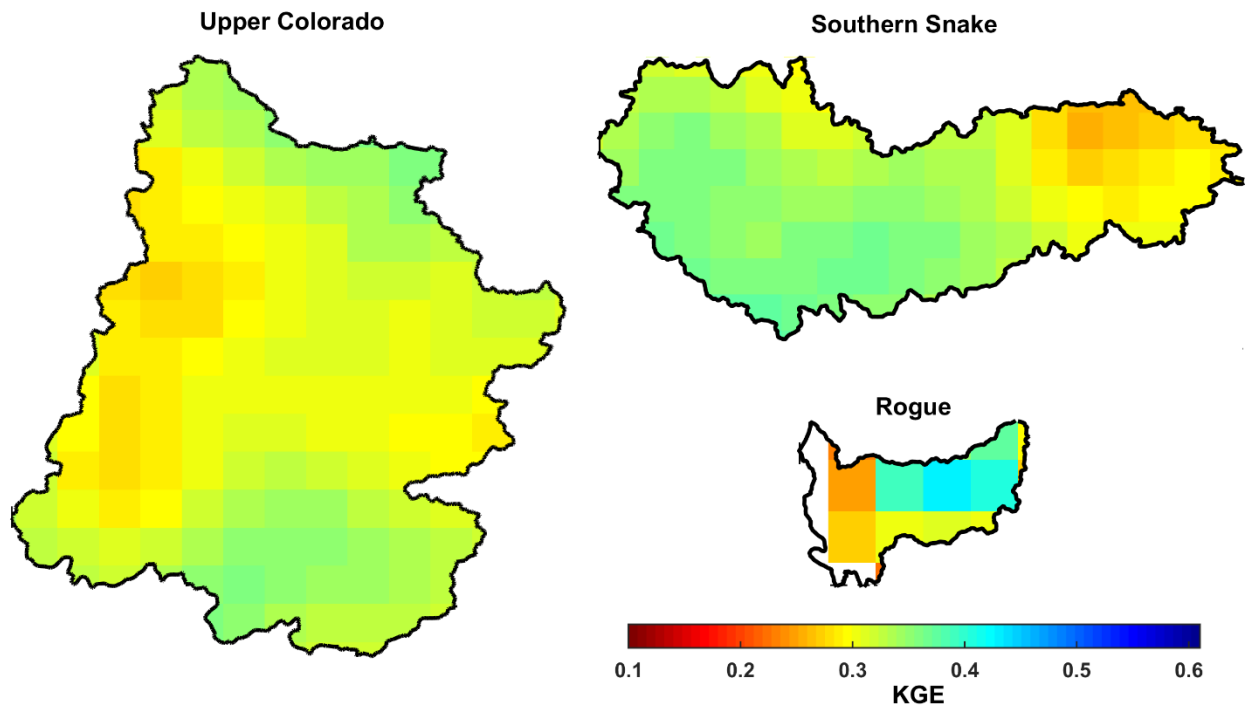


Figure 3. Kling-Gupta efficiency measure for the raw forecast during calibration period. White grid cells in Rouge River Basin present missing observations.

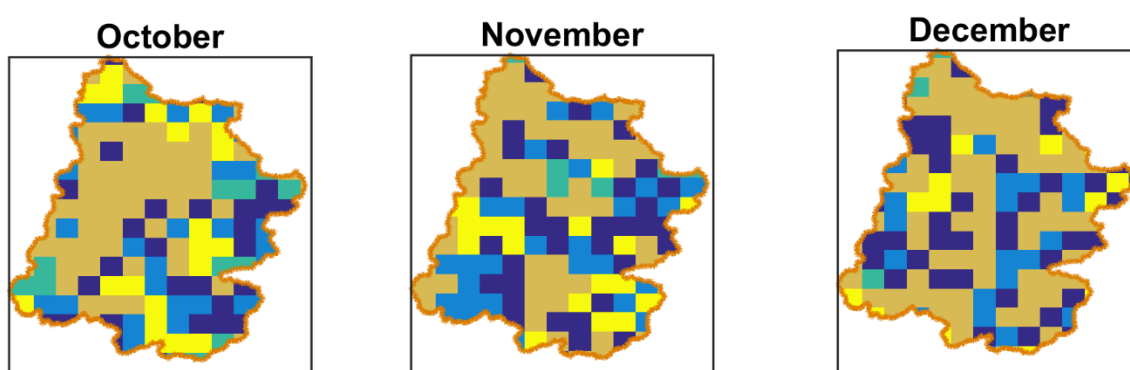
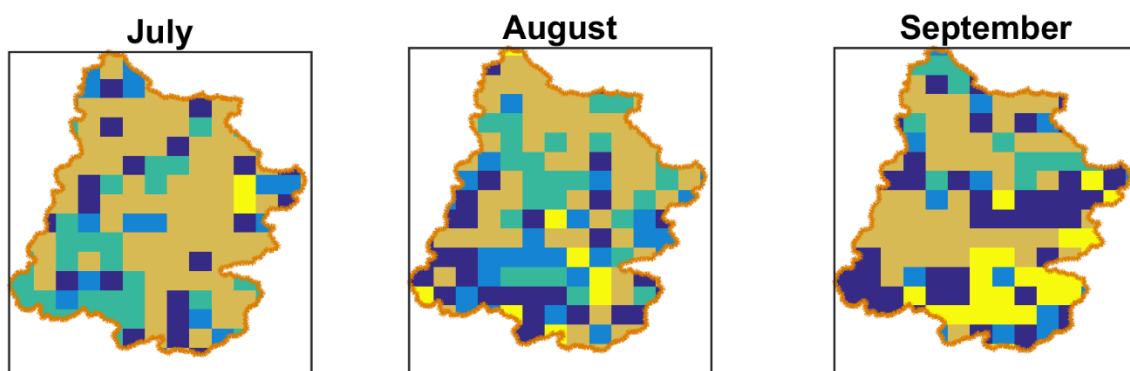
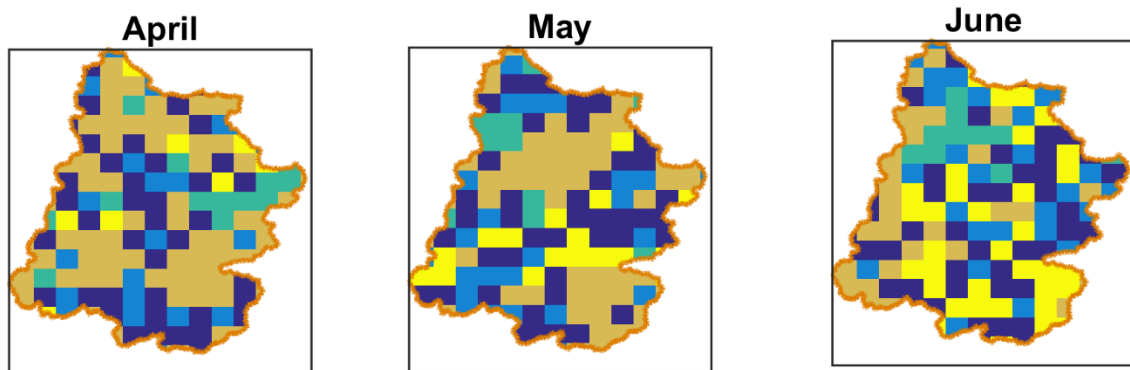
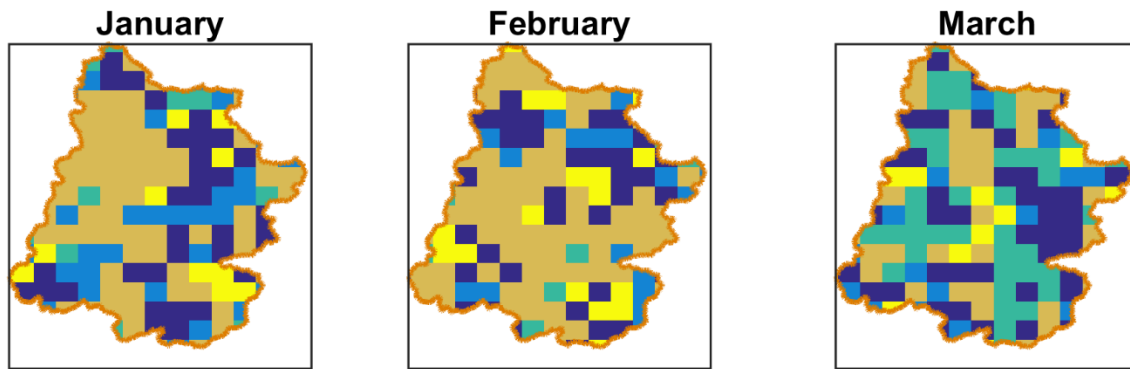


Figure 4. Selection of suitable copula functions for each grid cell across the Upper Colorado River Basin.

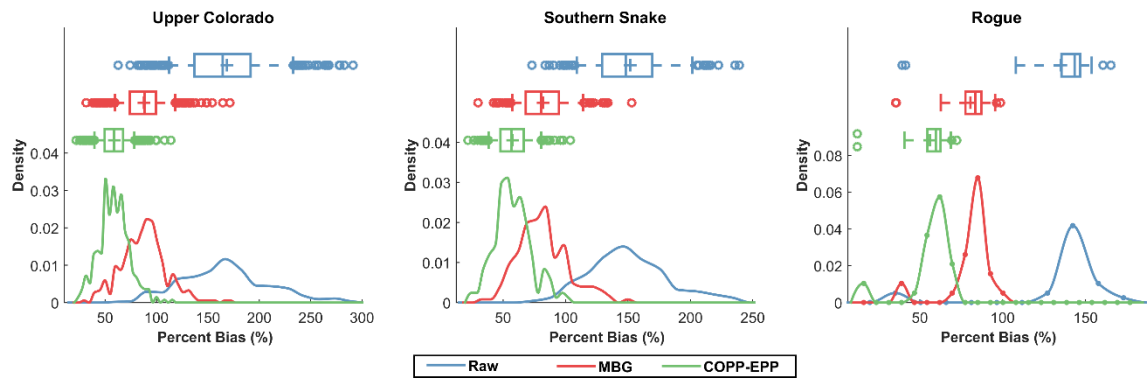


Figure 5. Absolute percent bias distribution over the three study basins. The bias is calculated for the raw forecast (blue line), and the ensemble mean from the MGB and COP-EPP outputs (red and green lines, respectively).

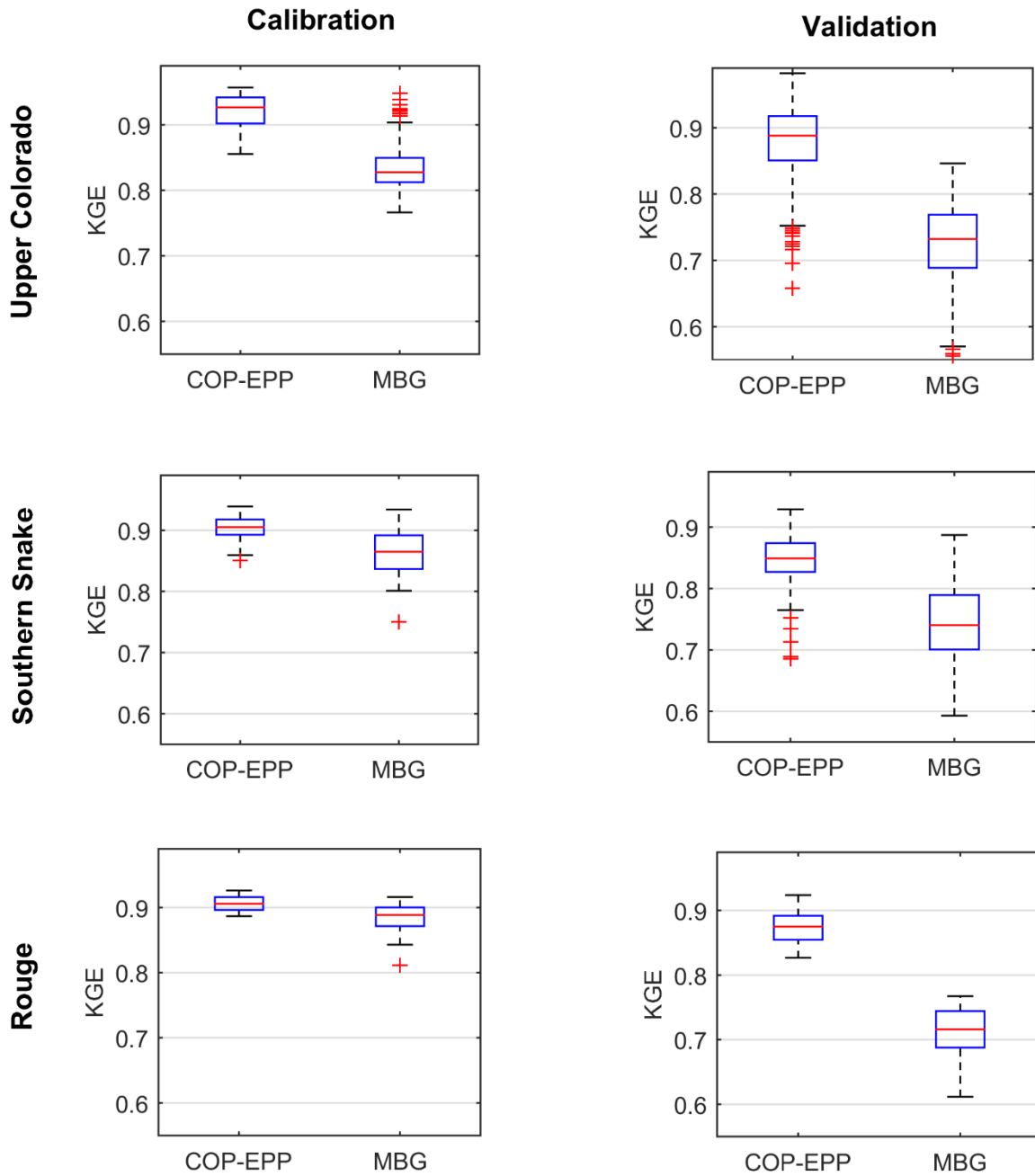


Figure 6. KGE measure calculated over the study basins after post-processing using the COP-EPP and MBG methods during calibration (left) and verification (right) periods.

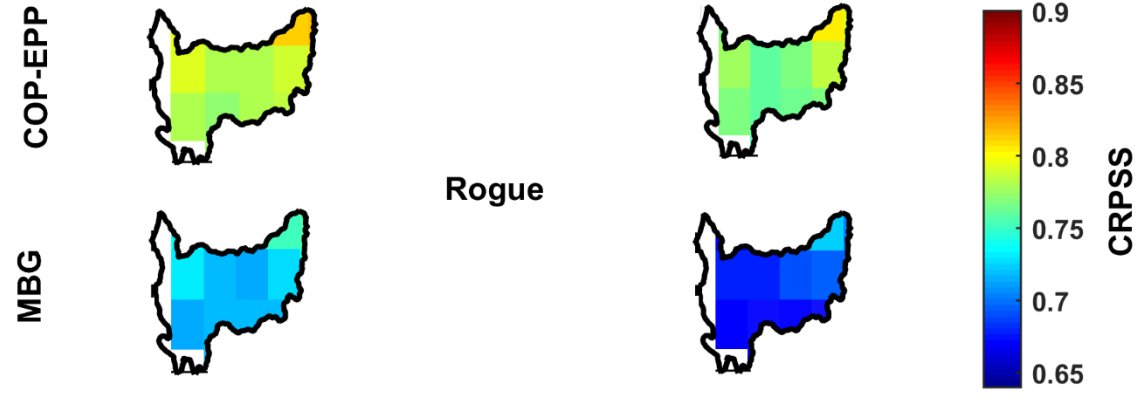
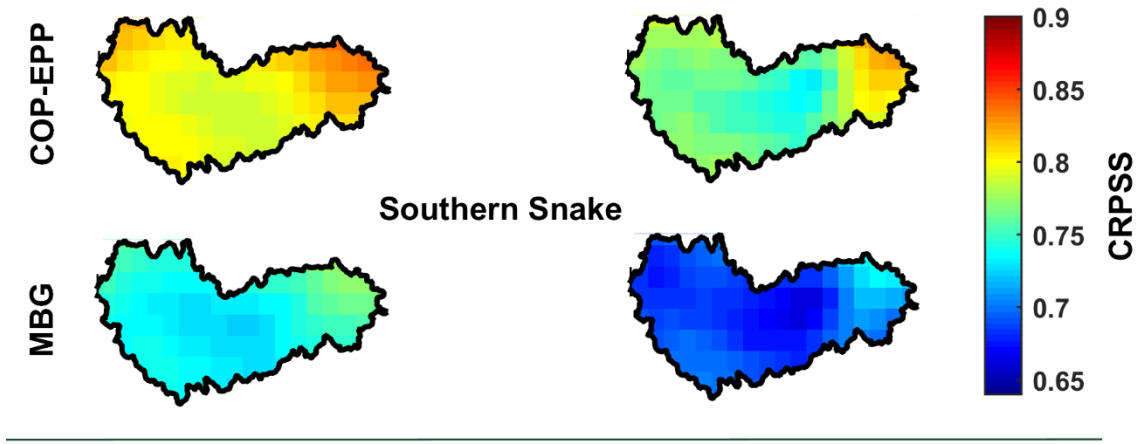
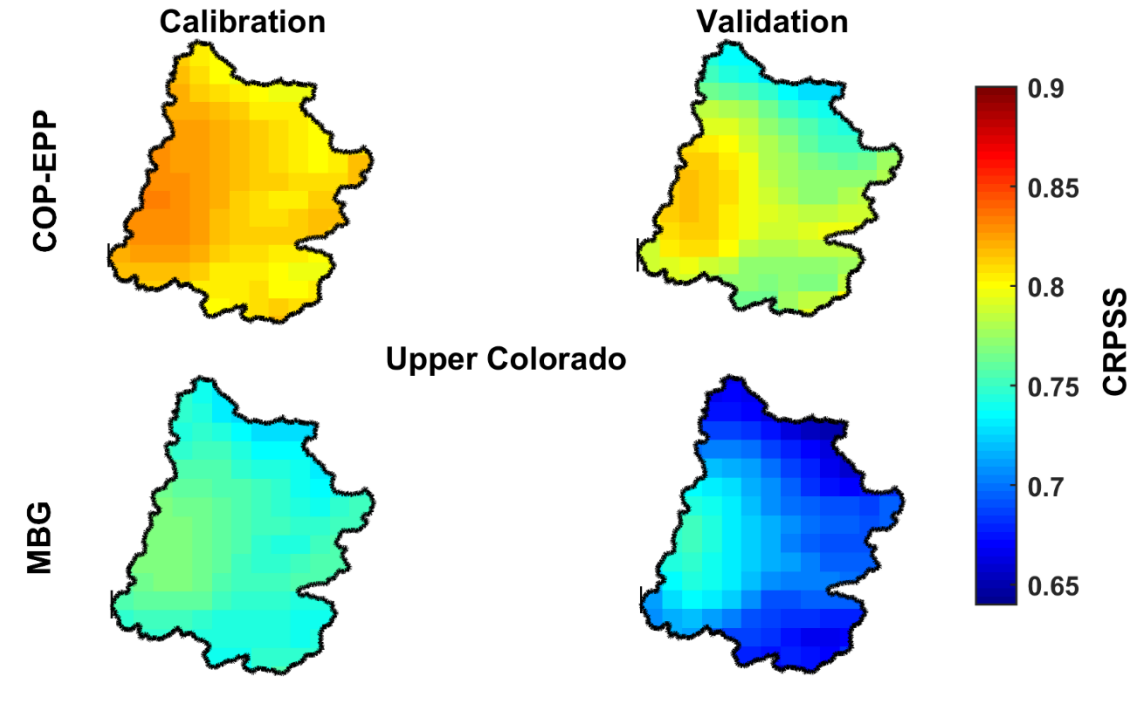


Figure 7. CRPSS measure calculated for 3 basins after implementing two post-processing methods for the calibration (left) and verification (right) periods.

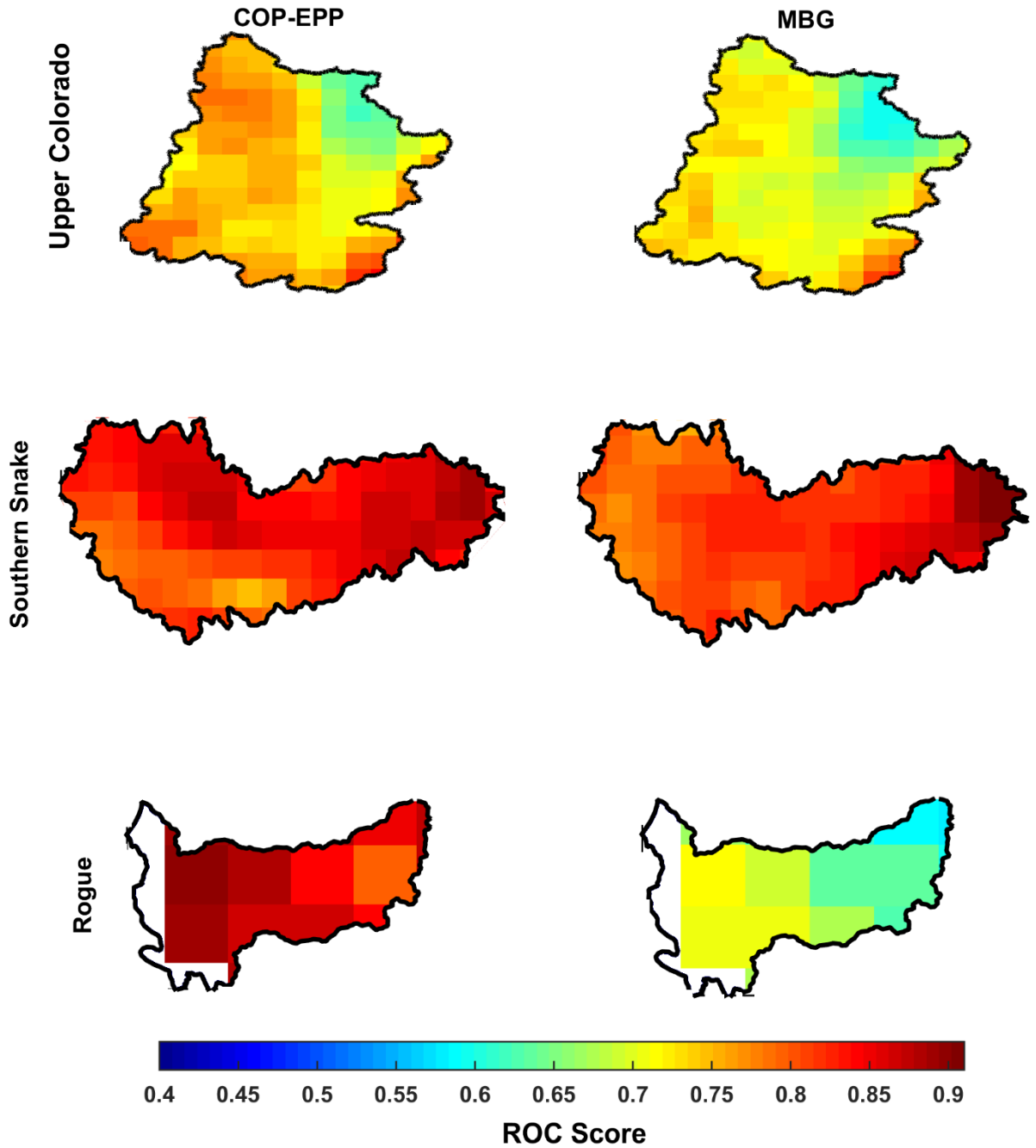


Figure 8. Assessment of forecast resolution based on ROC score for winter (Dec, Jan, and Feb) precipitation during verification period (2001-2014).

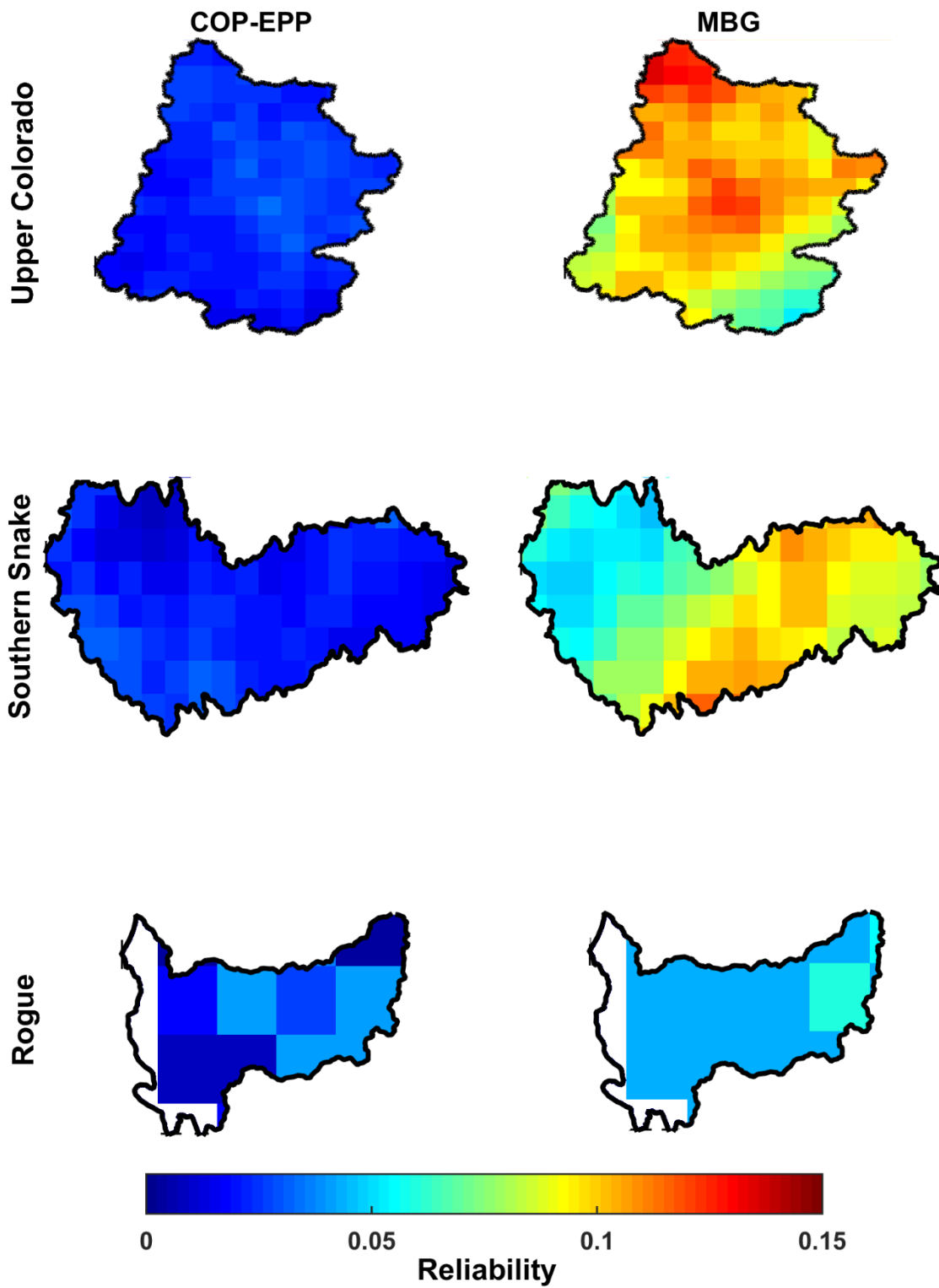


Figure 9. Reliability measure for winter precipitation (Dec, Jan, and Feb) calculated at 95th percentile of observation during the verification period (2001-2014). This measure ranges from 0 to 1 with the optimal value of 0.

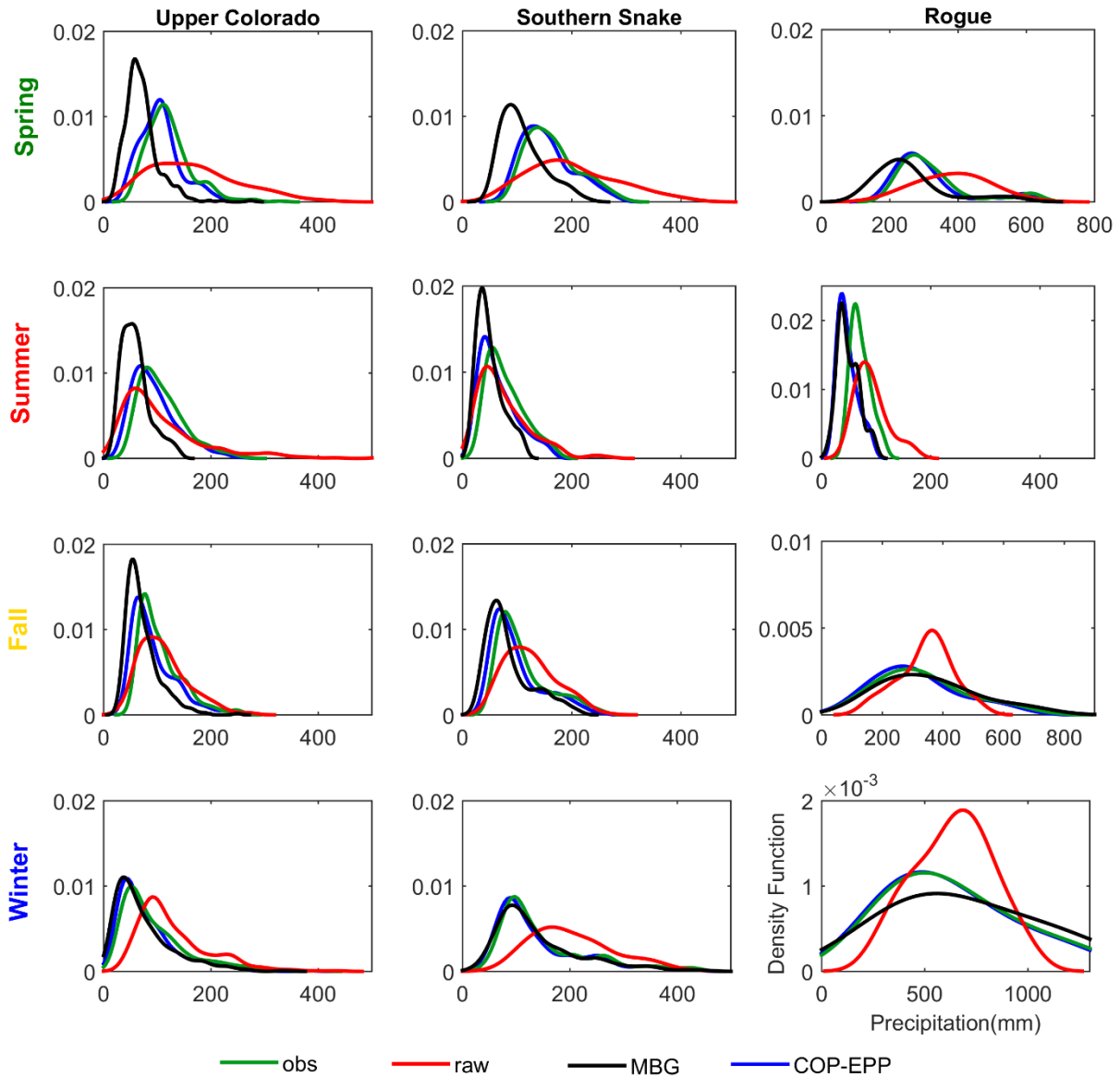


Figure 10. Probability density functions of seasonal precipitation from the observation, raw forecast, and most probable forecast based on the COP-EPP and MBG approach for three study basins. Seasonal precipitation is spatially averaged over all grid cells of each basin. Seasons are

categorized in the following order: Spring (Mar, Apr, and May), summer (Jun, Jul, and Aug), fall (Sep, Oct, and Nov), and winter (Dec, Jan, and Feb).

Table 1. Summary characteristics of the study basins

Basin Name	Drainage Area (km ²)	Annual Precipitation (mm)
Upper Colorado	280000	164
Southern Snake	180000	493
Rogue	5318	970